

Preparation and Characterization of Activated Carbon Spheres from Polystyrene Sulphonate Beads by Steam and Carbon Dioxide Activation

Arjun Singh,¹ Darshan Lal²

¹Terminal Ballistics Research Laboratory, Defence Research & Development Organisation, Ministry of Defence, Explosive Division, Sector 30-D, Chandigarh (UT) 160030, India

²Defence Materials & Stores Research & Development Establishment, DMSRDE, P. O., G. T. Road, Kanpur 13, Uttar Pradesh, India

Received 29 December 2008; accepted 21 August 2009

DOI 10.1002/app.31340

Published online 14 October 2009 in Wiley InterScience (www.interscience.wiley.com).

ABSTRACT: The polymeric precursor polystyrene sulphonate beads were used to produce activated carbon spheres (ACSs). ACSs were prepared by carbonization of polymeric precursor at 800°C followed by activation of resultant char with steam and carbon dioxide activation processes. The resulting ACSs were characterized for N₂ adsorption, Raman spectrometry, and scanning electron microscope (SEM). The adsorption properties such as, BET surface area (S_{BET}), pore volume (V_{pore}), and micropore volume (V_{micro}) of ACSs produced at different gasification time and temperature with steam and carbon dioxide activation were investigated in this study. It is found that porosity of ACSs produced from steam and carbon dioxide

activation increases with increasing activation time. The results exhibited that ACSs produced from above carbon dioxide activation have shown high S_{BET} and V_{pore} 1266 m²/g and 1.13 cm³/g respectively compared to ACSs from steam activation S_{BET} 949 m²/g and V_{pore} 0.98 cm³/g, respectively. SEM study revealed that ACSs produced from carbon dioxide activation have exhibited a smooth surface and better microstructure as compared to ACSs from steam activation process. © 2009 Wiley Periodicals, Inc. *J Appl Polym Sci* 115: 2409–2415, 2010

Key words: polystyrene sulphonate resin; activation; adsorption properties; microstructure

INTRODUCTION

In the present scenario of uncertainty of security of man and materials with reference to those chemical warfare by terrorists, versatile adsorbents are required to provide full protection against those toxic agents. Activated carbons have to play an important role as an adsorbent material for removal of toxic agents. Recently, the microporous activated carbons in spherical shape are used as strategic adsorbent materials for protection against organic toxic substances such as sulfur mustard, sarin, and soman which are toxic at parts per million concentrations.¹ For these applications, activated carbon spheres (ACSs) should possess not only higher BET surface area (S_{BET}), but also they have meso- (V_{meso}) and micropore volume (V_{micro}) and sufficient mechanical strength.² ACSs have an excellent durability and no abrasion due to their extremely hard shell. The standard samples of activated carbons in the form of powder or granules and activated fibers showed poor mechanical strength and lost important charac-

teristics after being processed in composite filter fabrics.^{3–5} The aforementioned materials used in filters layers, in foam or nonwoven showed a number of technical disadvantage as limited washability, low mechanical durability, little storage time, high insulation, limited adsorption capacity due to technical reasons. In chemical protective suits, activated carbons are fixed permanently on the textile carrier material by supporting base. ACSs eliminated all limitation because small percentage of outer surface of each sphere is in contact with the adhesive and making the largest part available for adsorption.

Recently, many polymers have been studied to produce activated carbons^{6–13} due to high carbon yield and low ash content. Moreover, the polymeric precursors have an advantage over natural ones that they can produce ACSs with higher adsorption capacity within reproducible pore size range by carefully choosing and controlling various parameters.¹⁴ For chemical protective device, many authors have reported to prepare ACSs from phenolic beads, polystyrene divinylbenzene, and pitch using physical activation.^{1,15–20} The physical activation consists of a carbonization step carbonization of raw materials followed by a step of activation of resulting char in the presence of activating agents such as steam or carbon dioxide.²¹

Correspondence to: A. Singh (arjunsng@yahoo.com).

The applicability of these materials mainly depends on the pore structure and its distribution. ACSs are highly porous amorphous solid structure and pores are scattered over a wide range of size and shape. According to IUPAC classification, the pores are divided into three groups by their sizes and assuming that pores are cylindrical in shape. Pores are classified according to pore width: micropores (size less than 2 nm), mesopores (between 2 and 50 nm), and macropores (more than 50 nm). It is reported that micropores contribute 90–95 % of the total surface area in activated carbons.²² The macropores are significantly not contributed to total surface area but these pores act as conduits for passage of the adsorbate into the interior or meso- and micropores surface. The type of microstructure determined by the choice of precursor, activation process, and control of processing conditions.²³ Microporous carbons are generally used in gas-phase adsorption because of the small gas molecules, whereas mesoporous carbons are mostly used in liquid-phase adsorption.⁴ In general, activated carbons both in granular and powdered forms are the most widely used adsorbents because of their excellent adsorption capacity for organic pollutants.²⁴

As far as selection of raw materials is concerned, they must be possessed high carbon content, low inorganic impurity, low volatile matter, and free from moisture and ash content. Other factors that determine the suitability of a raw material for ACSs production include ease of activation, bulk density, mechanical strength, cost, and ease of availability.

This work describes the preparation of ACSs from polystyrene sulphonate beads by carbonizing in N_2 atmosphere followed by activation by means of steam or carbon dioxide. The effects of process parameters, such as gasification time and temperature, on adsorption properties under study include S_{BET} , V_{pore} , and V_{micro} are investigated and discussed in this article. The ACSs are also evaluated for Raman spectrometry and scanning electron microscopy (SEM) technique.

MATERIALS AND METHOD

Material

Polystyrene sulphonate beads were received from ION Exchange Indian Ltd., were used as a precursor material for preparation of ACSs. Nitrogen and carbon dioxide gases used for process development of ACSs were procured from Oxygen Indian Ltd (India).

Preparation of ACSs

The polystyrene sulphonate beads with particle size range 0.6–1.2 mm were taken to prepare ACSs. The

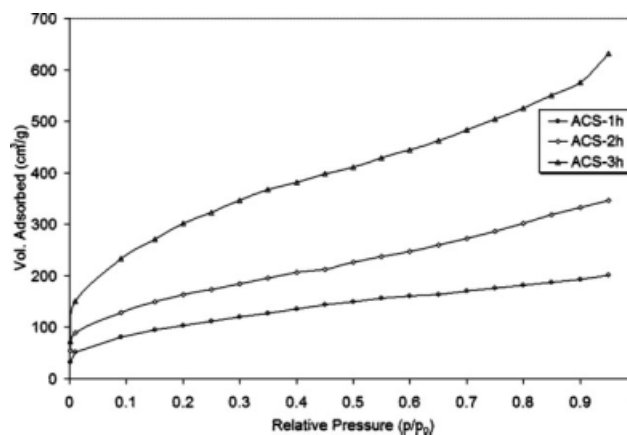


Figure 1 Adsorption isotherm of ACSs prepared at 800°C for different gasification times by steam activation.

polymeric beads were dried at 120°C for 5 h and then dried samples were carbonized in tubular quartz reactor with heating rate 10°C/min from room temperature to highest treatment temperature 800°C. The resulting carbonized beads were further activated with steam and carbon dioxide. The experiment sets of ACSs samples at different gasification times using carbon dioxide and steam activation were obtained as following: The samples ACS_{1h}, ACS_{2h}, and ACS_{3h} were prepared with steam activation at different gasification times 1, 2, and 3 h respectively, the samples ACS_{4h}, ACS_{6h}, and ACS_{8h} were prepared with carbon dioxide at temperature 850°C for gasification times 4, 6, and 8 h, respectively, and those at gasification temperatures represents of 750, 800, 850, and 900°C for 2 h with steam activation were designated as ACS₇₅₀, ACS₈₀₀, ACS₈₅₀, and ACS₉₀₀, respectively.

Characterization methods

To determine the surface characteristics parameters such as S_{BET} , and V_{pore} , adsorption isotherms of nitrogen molecule were recorded at $-196^{\circ}C$ on automatic instrument (Quantachrome Autosorb) computer controlled surface analyzer in relative pressure ranging from 10^{-3} to one. The Brunauer, Emmett, Teller (BET) equation was used to calculate the surface area.²⁵ Before measuring specific S_{BET} and pore structure parameters, the samples were out-gassed at 300°C in a vacuum oven for 3 h. The V_{micro} of the ACSs was determined from DR equation.²⁶ The total V_{pore} was obtained from the amount of nitrogen adsorbed at a relative pressure of 0.95 to the liquid nitrogen volume.²⁷ The subtraction of V_{micro} (from the DR equation) from the V_{pore} will give the V_{meso} . The surface morphology of ACSs was studied using a scanning electron microscope (Calro ZEISS). The samples were sputter coated with gold before analysis. The average pore size (or pore diameter) (D_{av}) of

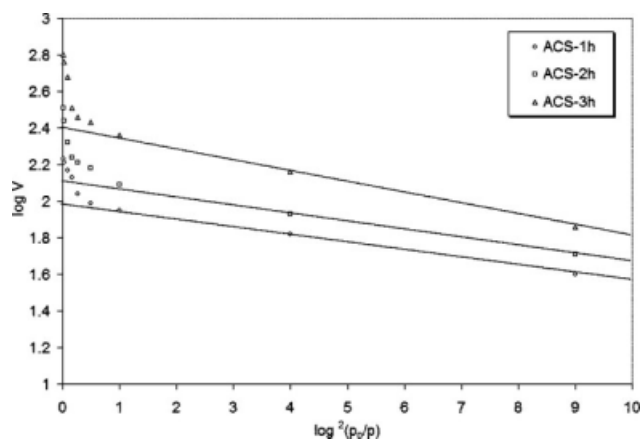


Figure 2 DR plot of ACSs obtained at temperature 850°C for different gasification time under steam activation.

ACSs was calculated from four times total V_{pore} (cm^3/g) over the corresponding specific S_{BET} (m^2/g) and it is assumed that pores are cylindrical shapes. The yield percentage of ACSs can be calculated from resultant sample weight to its initial polymer precursor weight. Raman spectra of ACSs were taken at room temperature under ambient conditions using a Renishaw Raman Microspore System which equipped with CCD detector. The 4–5 scans were given at a resolution of 4 cm^{-1} .

RESULTS AND DISCUSSION

ACSs from steam activation

Figure 1 shows that the adsorption capacity of ACSs increases with increase in gasification time from 1 to 3 h, which is indicating the increase of porosity upon activation. The N_2 adsorption isotherm of $\text{ACS}_{1\text{h}}$ exhibits that a large amount of N_2 is adsorbed remarkably at low relative pressure ($< 0.1 p/p_0$) and further there is very little N_2 adsorption of ACSs. Therefore, this isotherm can be considered as Type I for microporous carbons. Whereas N_2 adsorption isotherms of samples $\text{ACS}_{2\text{h}}$ and $\text{ACS}_{3\text{h}}$ show adsorption significantly take at high relative pressure, indicating change of N_2 adsorption isotherms from Type I to mixture of Type I and IV. These isotherms reflect that ACSs have micro and meso-porous nature according to Brunauer, Deming, Deming and Teller (BDDT) classification.²⁸ The ascending pattern observed after

the first point inflection increase from $\text{ACS}_{2\text{h}}$ to $\text{ACS}_{3\text{h}}$. This indicates that initial part of adsorption isotherm represents the micropore filling and further increase in nitrogen adsorption is due to multilayer formation followed by capillary condensation (mesopores filling and or capillary condensation). The microporosity of ACSs is determined using DR equation.²⁹ The DR is given as

$$V = V_0 \exp(-\{RT \log(p_0/p)/\beta E_0\}^2)$$

where V is the volume filled at temperature T and relative pressure p/p_0 , V_0 is total volume of the micropores, E_0 is characteristics adsorption energy for standard, β is the adsorbate affinity coefficient taken as 0.34 for nitrogen, and R is gas constant. Figure 2 shows the DR plots between $\log V$ versus $\log^2(p_0/p)$. The upward deviation points from linear DR plots at high values of relative pressure indicate the presence of mesopores. These results indicate the extents of gasification time with steam promote to mesopores formation.

Table I summarizes that the adsorption properties including S_{BET} , V_{pore} , V_{micro} , and D_p of prepared ACSs. The S_{BET} gradually increases with increase in gasification time from 1 to 3 h. The S_{BET} values are obtained from 310 to 949 m^2/g when gasification time varied from 1 to 3 h. The Table I also shows that V_{pore} and D_p increase from 0.27 to 0.98 cm^3/g and 3.5 to 4.1 nm when gasification time increases from 1 to 3 h, respectively. The yield percentage of ACSs continuously decreases from 10.7 to 5.4 with increase in gasification time from 1 to 3 h.

Effect of gasification temperature

The effect of gasification temperature on adsorption properties likes S_{BET} , V_{pore} and D_p of prepared ACSs from steam activation is summarized in Table II. The results show that gasification temperature is very important parameter for tailoring the pore structure of ACSs. It can be seen that the S_{BET} and V_{pore} of ACSs increase with increasing gasification temperature. The prepared ACSs exhibits a S_{BET} value ranging from 239 to 620 m^2/g when gasification temperature is varied from 750 to 900°C. The

TABLE I
ACSs Prepared from Polystyrene Sulphonate Beads at Temperature 850°C for Different Gasification Time by Steam Activation

ACSs sample	Time (h)	Burn-off (wt %)	Yield (wt %)	S_{BET} (m^2/g)	V_{pore} (cm^3/g)	$V_{\text{micro}}/V_{\text{pore}}$ (%)	D_p (nm)
$\text{ACS}_{1\text{h}}$	1	69.8	10.7	310	0.27	57	3.5
$\text{ACS}_{2\text{h}}$	2	78.4	8.1	547	0.51	50	3.7
$\text{ACS}_{3\text{h}}$	3	85.6	5.4	949	0.98	43	4.1

TABLE II
ACSs Prepared from Polystyrene Sulphonate Beads at Different Gasification Temperature for 2 h by Steam Activation

ACSs sample	Temperature (°C)	Burn-off (wt %)	Yield (wt %)	S_{BET} (m ² /g)	V_{pore} (cm ³ /g)	D_p (nm)
ACS ₇₅₀	750	71.4	10.7	289	0.26	3.6
ACS ₈₀₀	800	75.5	9.18	459	0.42	3.7
ACS ₈₅₀	850	78.4	8.1	547	0.51	3.7
ACS ₉₀₀	900	81.9	6.12	620	0.62	4.0

Table II shows that the V_{pore} of ACSs increases from 0.26 to 0.62 cm³/g with increase in gasification temperature from 750 to 900°C. The prepared ACSs at temperature 750°C show lower adsorption properties than ACSs obtained at higher gasification temperature 850°C, which indicates fast carbon gasification. The trend observed for adsorption properties and yields are found to be similar to the trend reported in the literature.³⁰ The Table II shows that the yield percentage of ACSs decreases with increase in gasification temperature from 750°C to 900°C. At high temperature, the activation of the char becomes more extensive, and thus this resulted in a low yield with widening the pore structure.

ACSs from carbon dioxide activation

Figure 3 shows the N₂ adsorption isotherms prepared ACSs at different gasification time by carbon dioxide activation. The N₂ adsorption isotherm of ACS_{4h} is sharp at low relative pressure and plateau is nearly horizontal at high relative pressure, which is a characteristic of Type I of isotherm according to [BDDT] classification. Thus, the prepared ACSs are mainly microporous. The N₂ adsorption isotherms of samples ACS_{6h} and ACS_{8h} show a progressive increase in adsorption at higher relative pressure, indicating that isotherms samples ACS_{6h} and ACS_{8h} are a mixture of Type I and Type IV. This also indicates widening of the micropores into mesopores, as referred from the opening of the knee of isotherm and higher slope of the plateau.

The adsorption properties of ACSs derived from N₂ adsorption isotherms are shown in Table III. The results show that the prepared ACSs exhibit a S_{BET} ranging from 566 to 1266 m²/g with gasification time increasing. It can be seen from Table III that the V_{pore} increases from 0.30 to 1.13 cm³/g when gasification time increases from 4 to 8 h. The yield percentage of ACSs decreases from 19.2 to 5.7 with increasing gasification time from 4 to 8 h. Figure 4 shows the DR plots between log V versus log²(p_o/p). The upward deviation points from linear DR plots at high values of relative pressure indicate the presence of mesopores. The upward deviation curve from linear DR plots increase with increasing gasification time, which indicates excess of the mesoporosity. Table III shows that the V_{micro} (%) of ACSs decreases

from 77.5 to 52.6% when extents of burn-off increases from 48.9 to 84.6 %.

It is known that the type of the porosity developed in ACSs depends on the type of precursor materials used and activation methods. The ACSs from novolac-type phenolic resin¹⁹ was activated to a high degree of burn-off 62% possessed S_{BET} 1663 m²/g and mesoporosity of 37%. Cai et. al.²² also attempted to prepare the ACSs from novolac-type phenolic resin as precursor by super critical water, which had a degree of carbon burn-off 50.8 %, possessed S_{BET} of 919 m²/g and mesoporosity of 17.0%. In contrast, ACSs prepared from polystyrene sulphate beads have shown S_{BET} of 1266 m²/g with mesoporosity of 57.8%, which had a degree of ACSs burn-off 84.6%. These adsorption properties are comparatively better than those of commercial available ACSs from pitch and novolac-type resin.²²

Comparison of activation methods

Figures 5 and 6 show the relationship between S_{BET} and yield (%) versus burn-off and relationship between V_{micro} (%) and V_{pore} versus extent of burn-off for ACSs obtained from carbon dioxide and steam activation, respectively. Burn-off is defined as the percentage solids after activation process³¹ which can be calculated from resultant sample weight to its initial carbon char weight obtained after carbonization. It can be seen that ACSs prepared from steam activation exhibit maximum S_{BET} value of 946 m²/g,

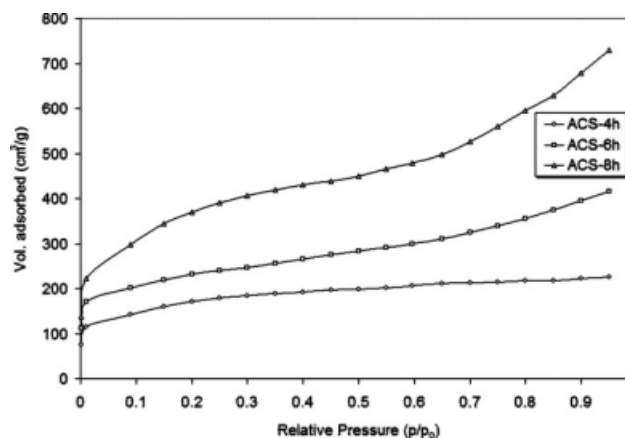


Figure 3 Adsorption isotherm of ACSs prepared at 850°C for different gasification time by carbon dioxide activation.

TABLE III
ACSs Prepared from Polystyrene Sulphonate Beads at Temperature 850°C for Different Gasification Time by Steam Activation

ACSs sample	Time (h)	Burn-off (wt %)	Yield (wt %)	S_{BET} (m^2/g)	V_{pore} (cm^3/g)	$V_{\text{micro}}/V_{\text{pore}}$ (%)	D_p (nm)
ACS _{4h}	4	48.9	19.2	566	0.36	77.5	2.6
ACS _{6h}	6	64.9	12.2	903	0.65	66.3	2.9
ACS _{8h}	8	84.6	5.7	1266	1.13	52.6	3.6

while ACSs prepared by carbon dioxide activation show higher S_{BET} value of $1266 \text{ m}^2/\text{g}$ at same extent of burn-off. Tables I and III show that a large D_p in the range 3.5 to 4.1 nm is obtained by steam activation, while ACSs obtained by carbon dioxide activation resulting D_p in range of 2.6 to 3.6 nm. This result revealed that ACSs produced from steam activation are a wider of pore sizes than those obtained from carbon dioxide activation, those differences in results due to different reactivity of carbon dioxide and steam with carbons which are responsible to control the competition between rates of diffusion and gasification reactions. Figure 5 shows the yield percentage of ACSs derived from carbon dioxide activation is better than ACSs from steam activation. Figure 6 show that the fraction of V_{micro} is located 0.78 to 0.52% for carbon dioxide activation is much larger than that of steam activation. It is concluded that ACSs from carbon dioxide activation have exhibited better adsorption properties and they are mainly microporous in nature than those prepared by steam activation.

Raman spectra of ACSs

Raman spectrometry is one of the most powerful tools to investigate structural information of carbon materials.³² Tuinstra and Koenig³³ first reported the first order Raman spectrum of a graphite single crystal. Figure 7 shows first order Raman spectra of ACSs samples (ACS_{6h}, and ACS_{8h} and ACS_{3h})

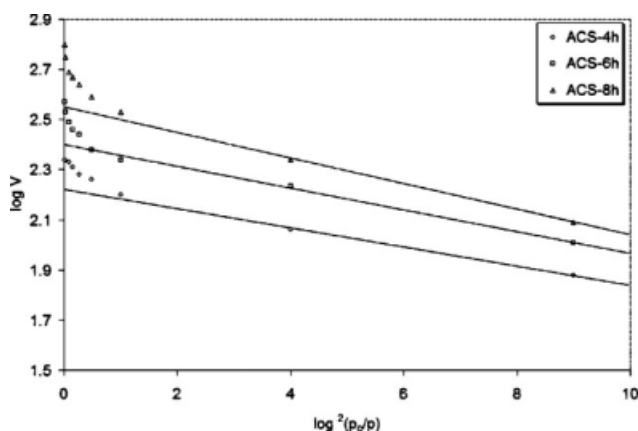


Figure 4 DR plot of ACSs obtained at temperature 850°C for different gasification time under steam activation.

obtained from carbon dioxide and steam activation. There are two specific absorption peaks locates within the $1593\text{--}95 \text{ cm}^{-1}$ (G-mode) and $1337\text{--}40 \text{ cm}^{-1}$ (D-mode), respectively. The G-mode peak refers the normal graphite structures and D-mode represents the short-range turbostratic structures.³⁴ ACS_{3h} obtained from steam activation exhibits peaks at 991 and 626 cm^{-1} in addition to G- and D-peaks which may be caused of functional groups due to carbon-H₂O reaction. Table IV listed the Raman band frequency, and full width at half maximum and intensity ratio of Raman D- and G-mode I_D/I_G (peak intensities) for ACSs samples. It can also be seen that the R value for samples ACS_{4h} and ACS_{8h} prepared from carbon dioxide activation increases with increase in activation time from 6 to 8 h, indicating more disorder carbon.

Surface morphology of ACSs by SEM

SEM micrographs of prepared ACSs using steam and carbon dioxide activation are compared in Figure 8. SEM image of ACSs prepared at temperature 800°C for 3 h by steam activation have shown in Figure 8(a) (ACSs at 2500×) and Figure 8(b) (ACSs at magnified 10,000×). It can be seen from Figure 8(a) that ACSs have a voids surface. The surface of ACSs is further magnified (10,000×) and image shows a large amount of interspaces in the order of meso- and micrometers, which indicates a highly disorganized porosity. While, ACSs developed from carbon

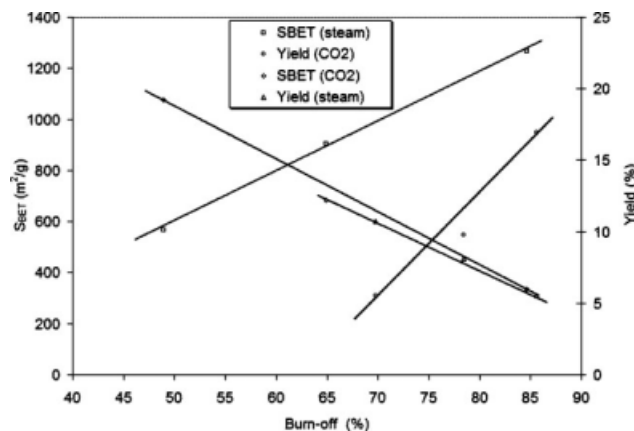


Figure 5 Comparison of S_{BET} and yield of ACSs prepared from steam and carbon dioxide activation with burn-off.

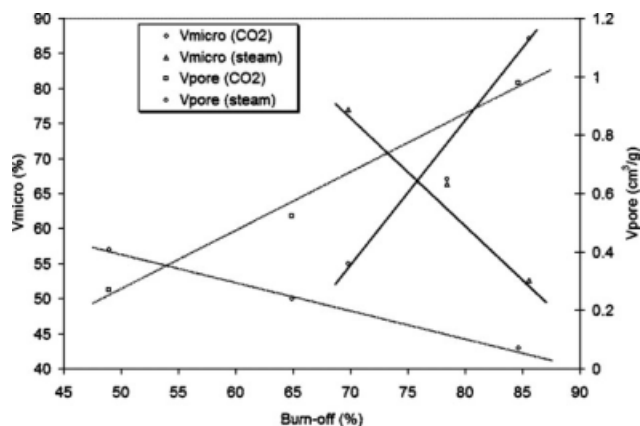


Figure 6 Comparison of V_{pore} and V_{micro} of ACSs prepared from steam and carbon dioxide activation processes with burn-off.

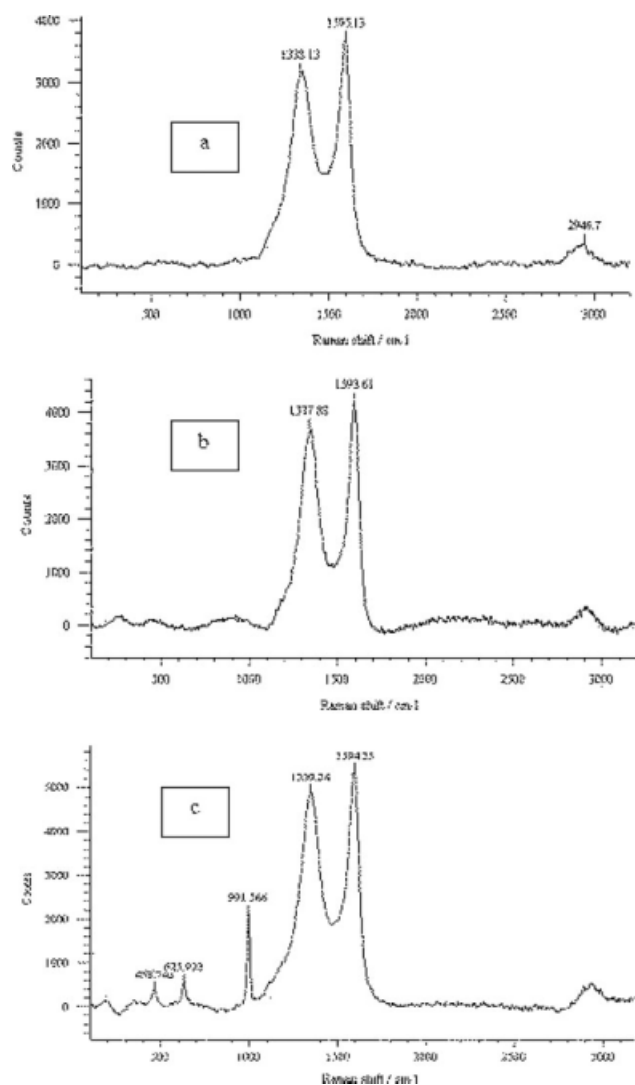


Figure 7 Raman spectra of ACSs prepared from carbon dioxide activation (a) ACS_{6h}, (b) ACS_{8h}, and (c) steam activation ACS_{3h}.

TABLE IV
Raman Spectra Analysis of ACSs Prepared from Carbon Dioxide and Steam

ACSs Sample	Burn-off (wt %)	G-peak		D-peak		$R^a = I_D/I_G$
		ν^b (cm ⁻¹)	Γ^c (cm ⁻¹)	ν^b (cm ⁻¹)	Γ^c (cm ⁻¹)	
ACS _{6h} (CO ₂)	48.9	1338.1	116.0	1595.1	66.3	0.83
ACS _{8h} (CO ₂)	84.7	1337.9	103.5	1593.6	60.9	0.84
ACS _{3h} (steam)	84.6	1339.8	106.0	1594.4	62.7	0.84

^a I_D/I_G is intensity of D over the intensity of G-peak.

^b ν indicate the Raman frequency of G- and D-peak.

^c Γ represents full width at half maximum G- and D-peak.

dioxide activation are quite different surface morphology and pore sizes than those prepared by steam activation. Figure 8 (c,d) shows that black shallow of pores are uniform well developed cavities on surface. SEM observations revealed that ACSs produced from carbon dioxide activation have a more compact surface and well-developed microstructure than those obtained from steam activation.

CONCLUSIONS

This study revealed that ACSs with higher S_{BET} was obtained from polystyrene sulphonate beads using physical activation. We have studied experimentally the effects of processing parameters such as, gasification time and temperature on adsorption properties of ACSs using steam and carbon dioxide activation. ACSs prepared at 850°C with steam and carbon dioxide activation show that the adsorption properties such as, S_{BET} , and V_{pore} increase with increasing gasification time. The ACSs prepared carbon dioxide activation have shown a high S_{BET} of 1266 m²/g with high V_{pore} of 1.13 cm³/g compared to S_{BET} 949 m²/g and V_{pore} 0.98 cm³/g by steam activation, respectively. These ACSs are microporous and the fraction of V_{micro} is decreased from 0.78 to 0.52 when gasification time is varied from 4 to 8 h. The porosity of ACSs is also found to increase with increase gasification temperatures from 850 to 1150°C. The Raman spectra shows that ACSs are not composed of short-range turbostratic structure. The SEM micrographs clearly show that the ACSs produced from carbon dioxide activation are well-developed microstructure and have a more compact surface than those from steam activation. It is concluded that ACSs prepared from carbon dioxide activation has shown better adsorption properties and yield compared to ACSs from steam activation method. These ACSs are quite useful in many

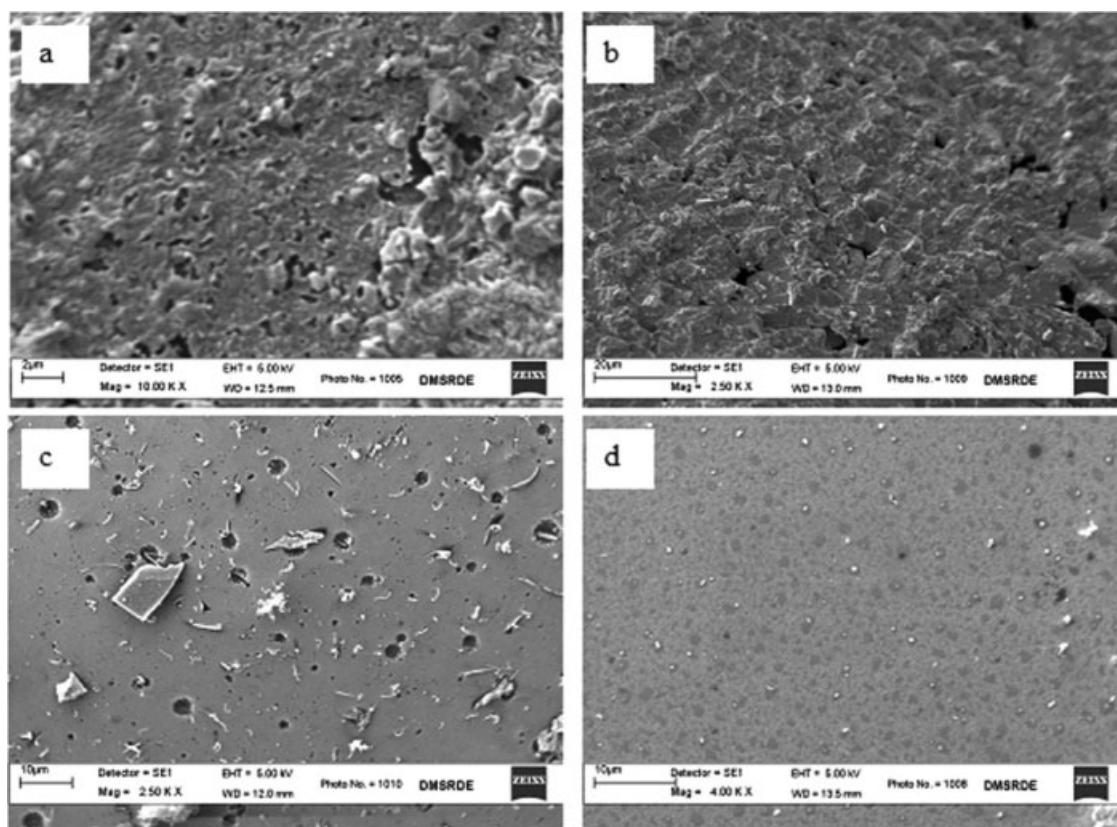


Figure 8 SEM micrographs of ACSs produced at different magnification: (a) ACSs at X 2500 and (b) the surface of the ACSs magnified $\times 10,000$ by steam activation (c) ACSs at $\times 2500$ (d) ACSs at higher magnified $\times 4000$ from carbon dioxide activation.

applications such as, pollution control, catalyst support, and protection against toxic substances.

The authors are thankful to Drs KUB Rao, Director, DMSRDE, Kanpur, Satish Kumar, Director, TBRL, Chandigarh, and Santosh Kumar Tripathi for their constant guidance and support. They also thank Sanjeevan Aggrawal for his help extended for BET Studies

References

- Yenisoy-Karakas, S. S.; Aygun, A.; Gunes, M.; Tahtasakal, E. *Carbon* 2004, 42, 477.
- Hu, Z.; Srinivasan, M. P. *Micropo Mesopor Mater* 2001, 43, 267.
- Tamai, H.; Kakii, T.; Hirota, Y.; Kumamoto, T.; Yasuda, H. *Chem Mater* 1996, 8, 454.
- Liu, Z. C.; Ling, L. C.; Qiau, W. M.; Liu, L. *Carbon* 1999, 37, 663.
- Gurudatt, K.; Tripathi, V. S. *Carbon* 1998, 36, 1371.
- Jain, M. K.; Balasubramanian, H.; Desai, D. J. *Mater Sci* 1987, 22, 301.
- Centeno, T. A.; Fuertes, A. B. *Carbon* 2000, 38, 1067.
- Tennison, S. R. *Appl Catal A* 1998, 173, 289.
- Takecichi, T.; Yamazaki, Y.; Zuo, M.; Ito, A.; Matsumoto, A.; Inagaki, M. *Carbon* 2000, 39, 257.
- Lahaye, J.; Nanse, G.; Bagreev-Strelko, V. *Carbon* 1999, 37, 585.
- Hu, Z.; Srinivasan, M. P.; Ni, Y. *Carbon* 2001, 39, 877.
- Kocirik, M.; Brych, J.; Hradil, J. *Carbon* 2001, 39, 1919.
- Tanaike, O.; Fukuoka, M.; Inagaki, M. *Synth Met* 2002, 125, 255.
- Tsai, W. T.; Chang, C. Y.; Wang, S. Y.; Wang, C. F.; Chim, S. F.; Sun, H. F. *Resour Conserv Recycl* 2001, 32, 43.
- Bacaoui, A.; Yaacoubi, A.; Dahbi, A.; Bennoouna, C.; Plan T-Luu, R.; Maldonado-Hodar, F. F. *Carbon* 2001, 39, 425.
- Linares-Castello, D.; Lillo-Rodenas, M. A.; Cazorla-Amoros, D.; Linarres-Solano, A. *Carbon* 2001, 39, 741.
- Srinivasa Kannan, C.; Bakar, M. A. *Biomass Bioenergy* 2004, 27, 89.
- E-Genndi, M. S. *Adsorp Sci Technol* 1997, 15, 777.
- Yang, J. B.; Ling, C.; Liu, L.; Kang, F. Y.; Huang, Z. H.; Wu, H. *Carbon* 2002, 40, 911.
- Singh, A.; Lal, D. *J Appl Polym Sci* 2008, 110, 3283.
- Singh, G. S.; Lal, D.; Tripathi, V. S. *J Chrom A* 2004, 1036, 189.
- Cai, Q.; Huang, Z. H.; Kang, F.; Yang, J. B. *Carbon* 2004, 24, 775.
- Zhu, Z.; Li, A.; Zhong, S.; Liu, F.; Zhang, Q. *J Appl Polym Sci* 2008, 109, 1692.
- Rodriguez-Reinoso, F.; Marsh, H.; Heintz, E. A., Eds. *Introduction to Carbon Technologies, Handbook*; University of Alicante: Alicante Spain, 1997; p 35
- Gregg, S.; Sing, K. S. W. *Adsorption, Surface Area and Porosity*; Academic Press: London, 1982; pp 42–112.
- Gregg, S.; Sing, K. S. W. *Adsorption, Surface area and Porosity*; Academic Press: London, 1982; pp 195–257.
- Freeman, J. J.; Gimblett, F. G. R.; Sing, K. C. W. *Carbon* 1989, 27, 7.
- Brunauer, S.; Demnig, L. S.; Dening, W. S.; Teller, E. *J Am Chem Soc* 1940, 62, 1723.
- Dubinin, M. M. *Carbon* 1998, 27, 457.
- Teng, H.; Wang, S. C. *Carbon* 2000, 38, 817.
- Yag, S. H.; Hu, G. *Carbon* 2002, 40, 277.
- Sadezky, A.; Muchenhubar, H.; Grothe, H.; Niessener, R. *Carbon* 2005, 43, 173.
- Tuinstra F, F.; Koenig, J. L. *J Chem Phys* 1970, 53, 1126.
- Lespade, P.; Marchand, A.; Couzi, M.; Cruege, F. *Carbon* 1964, 22, 375.